Determining fast-ion velocity-space distribution functions using velocity-space tomography

A.S. Jacobsen[1], M. Salewski[1], B. Geiger[2], L. Stagner[3], J. Eriksson[4], S.K. Nielsen[1], W.W. Heidbrink[3], S.B. Korsholm[1], F. Leipold[1], J. Rasmussen[1], M. Stejner[1], M. Weiland[2] and the ASDEX Upgrade Team

[1] *Technical University of Denmark, Department of Physics, Kgs. Lyngby, Denmark*

[2] *Max Planck Institute for Plasma Physics, Garching, Germany*

[3] *University of California Irvine, Irvine, CA, USA*

[4] *Department of Physics and Astronomy, Uppsala University, Sweden*

Introduction

In a burning plasma the heating comes from the very fast fusion products themselves. To ensure effective heating, the fusion products must be sufficiently confined until they have transferred their energy to the bulk plasma. Therefore, studies of the confinement of fast ions in current fusion devices are important. This includes studies of the interplay between fast ions and plasma instabilities.

Using velocity-space tomography it is possible to infer the fast-ion velocity-space distribution function directly from measurements [1, 2, 3, 4]. This is done by combining measurements from several fast-ion detectors measuring in the same location in position space. Velocity-space tomography requires knowledge about the velocity-space sensitivity of the fast-ion diagnostics. This sensitivity is described by so-called velocity-space weight functions. These have been formulated for fast-ion D_α (FIDA) spectroscopy [5, 6], collective Thomson scattering (CTS) [7], neutron emission spectrometry (NES) [8, 9], γ-ray spectroscopy (GRS) [10] and neutral particle scattering (NPA) [11]. A weight function, w, relates a fast-ion measurement, s, to the full fast-ion velocity distribution function, f.

$$s = \iint w f \, \mathrm{d}E \mathrm{d}p, \tag{1}$$

where the integration is with respect to energy and pitch. The pitch is here defined as $\frac{v_\parallel}{v}$ with positive sign in the direction of positive toroidal current. $v_\parallel$ is the velocity parallel to the magnetic field and v is the speed of the ion. Equation (1) can be discretized giving a linear set of equations:

$$S = WF. \tag{2}$$

The goal is now to calculate F from equation (2). However, this is mathematically an ill-posed inverse problem which can only give sensible results if the problem is regularized. There exist

many different ways to regularize inverse problems. In the example shown in this paper we use truncated singular value decomposition. This is effectively a filtering method which removes the finer details in the solution suppressing the effect of the noise in the measurements.

Tomography of a sawtooth crash

FIDA spectroscopy measures Doppler-shifted light emitted by excited fast neutrals right after they have undergone charge exchange with injected NBI ions. Here, we present results of velocity-space tomographies using coherently averaged measurements taken just before and just after sawtooth crashes in discharge #30815 in the ASDEX Upgrade tokamak [2]. In this discharge we measured FIDA light in four different views. Each view consists of several lines of sight measuring in different locations in position space. Each view has a line of sight that intersects the NBI beam at the same location in the plasma center, each with a different angle to the magnetic field. The angle between the local magnetic field and the line of sight determines the projection direction of the velocity distribution and therefore determines the velocity-space sensitivity and thus the shape of the weight functions [6]. The measurement volume is located around $\rho_t = 0.1$, well within the sawtooth inversion radius located near $\rho_t = 0.3$. Figure 1(a) shows a tomography of the fast-ion velocity distribution function calculated using FIDA spectra measured right before a sawtooth crash. Figure 1(c) shows a theoretical distribution calculated using TRANSP/NUBEAM [12]. The shaded region at low energies correspond to low Doppler shifts in the FIDA spectra. Here the FIDA light cannot be observed as the halo, the beam emis-

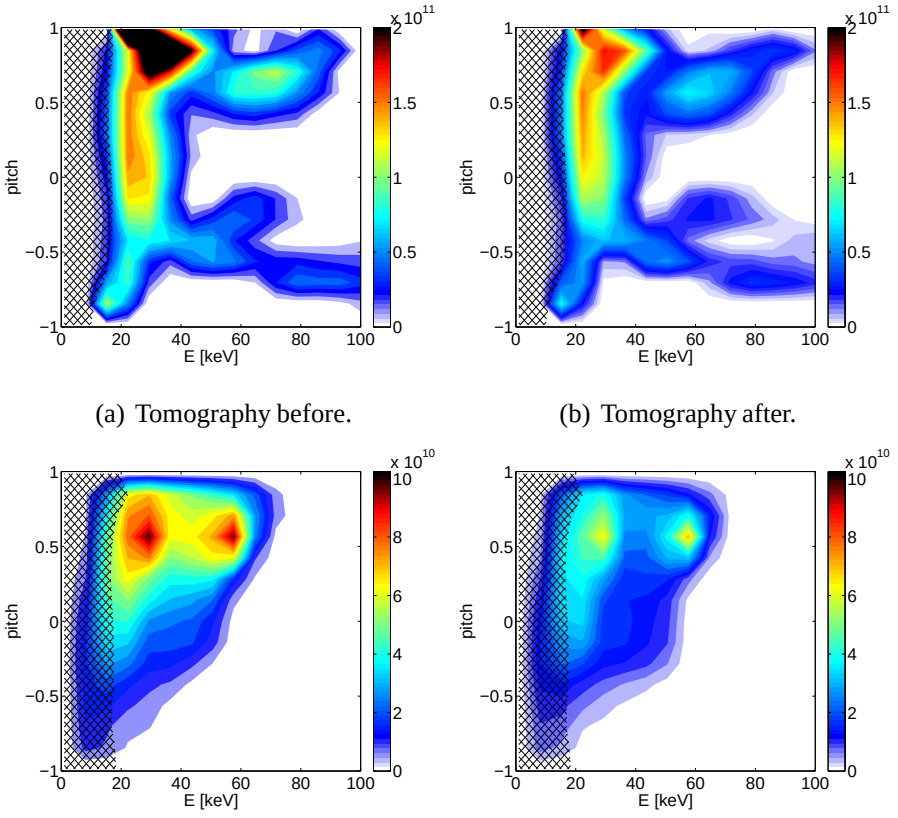

(a) Tomography before. (b) Tomography after.

(c) TRANSP before. (d) TRANSP after.

Figure 1: Central fast-ion velocity distribution functions before and after a sawtooth crash in units of [ions/keV/cm^3].

sion and the cold D-alpha light are much stronger [13]. Several similarities between figures 1(a) and 1(c) are evident. Most ions have a positive pitch and the NBI full-energy peak at 60 keV can be seen. However, several discrepancies are evident as well, especially the $E > 40$ keV feature at a pitch around -0.5. This is most likely an artefact introduced by the inversion. The FIDA data in this discharge contain impurity lines which obscure parts of the spectra with large Doppler-shifts which might have been able to suppress this artefact through a measured lack of FIDA light.

Figure 1(b) shows a tomography calculated using data measured right after the sawtooth crash. Figure 1(d) shows the corresponding TRANSP/NUBEAM calculation. A clear drop in the distributions can be seen. Furthermore, the drop in the fast-ion distribution is larger for passing ions compared to trapped ions. To investigate this effect further, the relative change is calculated as $\frac{F_{before}-F_{after}}{F_{before}}$. Figure 2 shows the relative change as a function of pitch for two different energies. Trapped ions with pitch values around 0 are redistributed less than passing ions with pitch close to 1. This behaviour has also been observed on other machines [14]. For comparison, the relative change predicted by the Kadomtsev model implemented in TRANSP is also shown.

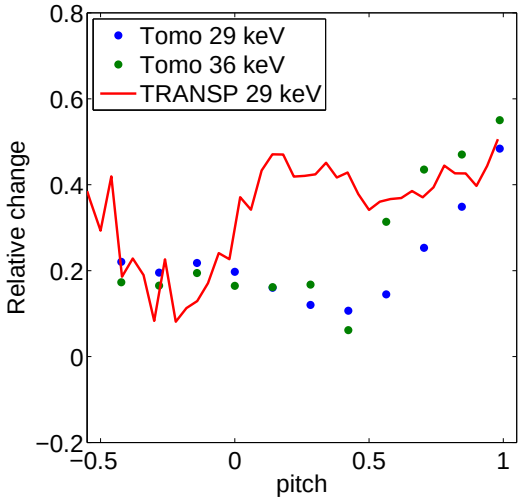

Figure 2: Relative change in fast ion density as a function of pitch for two different energies.

Discussion

As we mentioned in the introduction, the regularization of an inverse problem is essential in order to achieve sensible results. Many different regularization methods exists. The result depends on the choice of regularization and it should therefore preferably be made based on knowledge or assumptions about the true solution. A comparison of inversion methods for velocity-space tomography will be presented elsewhere.

The inversions can be improved by combining several different types of fast-ion diagnostics. For example, the FIDA views at ASDEX Upgrade could be combined with the CTS, NPA and NES diagnostics. In addition to the benefits gained by including more measurements, the different diagnostics yield complimentary information about fast-ion velocity space even if their projection angle is the same. Examples of weight functions for FIDA, CTS and NES are shown in figure 3, all calculated with a projection angle of 14°. The weight functions are plotted as a function of $v_{\|}$ and $v_{\perp}$ as the differences are more clear in these coordinates. The FIDA

and CTS weight functions have triangular shapes while the NES weight function is circular.

Conclusion

We have presented results of velocity-space tomography on a sawtooth crash at ASDEX Upgrade as an example of an application of the method. Using velocity-space tomography it is possible to recreate the full fast-ion velocity distribution function based on a combination of measurements from different detectors, each only measuring a projection of the distribution function. Our tomographic inversion suggests that passing ions are more affected by the sawtooth crash than trapped ions.

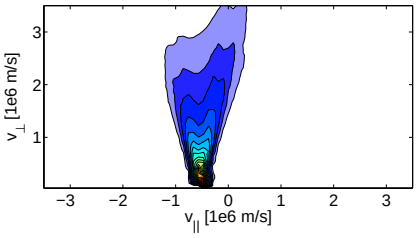

(a) FIDA.

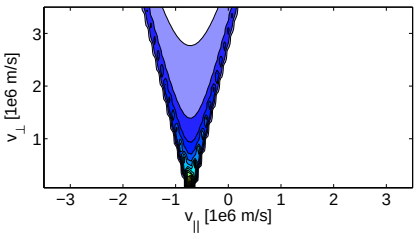

(b) CTS.

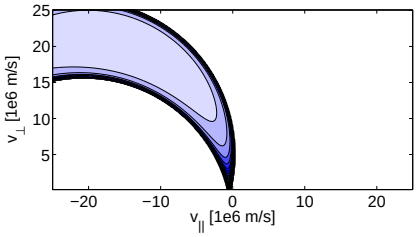

(c) NES.

Figure 3: Examples of FIDA, CTS and NES weight functions.

Acknowledgement

This work has been carried out within the framework of the EUROfusion Consortium and has received funding from the Euratom research and training programme 2014-2018 under grant agreement No 633053. The views and opinions expressed herein do not necessarily reflect those of the European Commission.

References

[1] M. Salewski et al., Nuclear Fusion **54**, 023005 (2014)

[2] B. Geiger et al., accepted in Nuclear Fusion, title: *Fast-ion transport and neutral beam current drive in ASDEX Upgrade*, (2015)

[3] M. Salewski et al., Nuclear Fusion **52**, 103008 (2012)

[4] M. Salewski et al., Nuclear Fusion **53**, 063019 (2013)

[5] W.W. Heidbrink et al., Plasma Physics and Controlled Fusion **49**, 1457-1475 (2007)

[6] M. Salewski et al., Plasma Physics and Controlled Fusion **56**, 105005 (2014)

[7] M. Salewski et al., Nuclear Fusion **51**, 083014 (2011)

[8] A.S. Jacobsen et al., Nuclear Fusion **55**, 053013 (2015)

[9] A.S. Jacobsen et al., Review of Scientific Instruments **85**, 11E103 (2014)

[10] M. Salewski et al., submitted, title: *Velocity-space sensitivity of high-resolution two-step reaction γ-ray spectroscopy*

[11] W.W. Heidbrink et al., Plasma Physics and Controlled Fusion **56**, 095030 (2014)

[12] A. Pankin et al., Computer Physics Communications **159**, 157-184 (2004)

[13] B. Geiger et al., Review of Scientific Instruments **84**, 113502 (2013)

[14] S.K. Nielsen et al., Nuclear Fusion **51**, 063014 (2011)